



Quantum dot resonant tunneling diode single photon detector with aluminum oxide aperture defined tunneling area

Li, H.W.; Kardynal, Beata; Ellis, D.J.P.; Shields, A.J.; Farrer, I.; Ritchie, D.A.

Published in:
Applied Physics Letters

Link to article, DOI:
[10.1063/1.2978232](https://doi.org/10.1063/1.2978232)

Publication date:
2008

Document Version
Publisher's PDF, also known as Version of record

[Link back to DTU Orbit](#)

Citation (APA):
Li, H. W., Kardynal, B., Ellis, D. J. P., Shields, A. J., Farrer, I., & Ritchie, D. A. (2008). Quantum dot resonant tunneling diode single photon detector with aluminum oxide aperture defined tunneling area. *Applied Physics Letters*, 93(15), 153503. <https://doi.org/10.1063/1.2978232>

General rights

Copyright and moral rights for the publications made accessible in the public portal are retained by the authors and/or other copyright owners and it is a condition of accessing publications that users recognise and abide by the legal requirements associated with these rights.

- Users may download and print one copy of any publication from the public portal for the purpose of private study or research.
- You may not further distribute the material or use it for any profit-making activity or commercial gain
- You may freely distribute the URL identifying the publication in the public portal

If you believe that this document breaches copyright please contact us providing details, and we will remove access to the work immediately and investigate your claim.

Quantum dot resonant tunneling diode single photon detector with aluminum oxide aperture defined tunneling area

H. W. Li,^{1,a)} B. E. Kardynał,^{1,3,b)} D. J. P. Ellis,¹ A. J. Shields,¹ I. Farrer,² and D. A. Ritchie^{2,a)}

¹Toshiba Research Europe Limited, Cambridge Research Laboratory, 208 Cambridge Science Park, Milton Road, Cambridge CB4 0GZ, United Kingdom

²Cavendish Laboratory, University of Cambridge, J. J. Thomson Avenue, Cambridge CB3 0HE, United Kingdom

³DTU Fotonik, Department of Photonics Engineering, Ørsted Plads 343, 2800 Kgs. Lyngby, Denmark

(Received 7 May 2008; accepted 31 July 2008; published online 14 October 2008)

Quantum dot resonant tunneling diode single photon detector with independently defined absorption and sensing areas is demonstrated. The device, in which the tunneling is constricted to an aperture in an insulating layer in the emitter, shows electrical characteristics typical of high quality resonant tunneling diodes. A single photon detection efficiency of $2.1\% \pm 0.1\%$ at 685 nm was measured corresponding to an internal quantum efficiency of 14%. The devices are simple to fabricate, robust, and show promise for large absorption area single photon detectors based on quantum dot structures. © 2008 American Institute of Physics. [DOI: 10.1063/1.2978232]

A strong interest in practical single photon detectors is stimulated by the development of quantum information technology¹ and an increasing demand for low light level detection. The most widely used single photon detectors at telecommunication and visible light wavelengths include avalanche photodiodes and photomultiplier tubes.^{2,3} Bolometers, superconductor nanowire detectors,⁴ and single quantum dot detectors⁵ can be used to extend the single photon detection to far-infrared range. It has also been shown that field-effect transistors^{6,7} and resonant tunneling diodes^{8,9} (RTD) containing a layer of self-assembled quantum dots (QDs) can detect single photons and their temperatures of operation is at least 77 K.^{10,11}

The detection of a single photon in QDs based RTD (QDRTD) devices results from a capture of a photohole in a single dot, which in turn modulates the resonant current through the device. The cross-wire geometry has been employed to realize small tunneling area devices⁸ necessary for single photon detection. In such devices, contacts have a form of a few micron (or less) wide semiconductor wires, which limit the operation of high current density RTDs by contributing strongly to series resistance, which suppresses single photon signal. In addition the light absorption area is defined by the small overlap between the contacts and this poses a serious limitation on detector applications.

We report in this letter the development of QDRTD detector, where we constrict the tunneling area in an otherwise large area detector in a separate lithographic step. This opens the possibility for realization of robust QDRTD single photon detectors with large absorption area. The device structure is shown schematically in Fig. 1(a).

The detectors are fabricated on wafers grown by molecular beam epitaxy on a semi-insulating GaAs substrate. The RTD structure of the wafer consists of a 10 nm GaAs quantum well confined between two 6 ML thick AlAs barriers with *n*-doped emitter and collector. Between the RTD and collector contact there is a 100 nm thick GaAs photon ab-

sorber. InAs QDs are placed in the absorber of the device 2 nm away from the AlAs tunneling barrier. Within emitter contact layers, 150 nm away from AlAs barrier, there is a 40 nm *n*⁺-AlAs layer for wet oxidation.

Fabrication of the device started from wet etching of mesas of $30 \times 30 \mu\text{m}^2$ down to the emitter contact layers. Wet oxidation was performed to convert the *n*⁺-AlAs layer into aluminum oxide (AlO_x), leaving an unoxidized aperture in the center.¹² The aperture defines the electron tunneling area of the device. The fabrication was completed by forming ohmic contacts to both emitter and collector contact layers. An optical image of the device is shown in Fig. 1(b) with the light spot marking the position of the aperture.

The current-voltage characteristics of the device were measured at 4.5 K. The result is shown in Fig. 2. For positive polarity of bias applied to the collector, an electric field is developed across the *i*-region of the device that allows photon detection.⁸ The high quality of the device manifests itself in a good definition of the resonance with high peak-to-valley current ratio and a clear phonon replica of the resonance. The effective tunneling area of the device was estimated by comparing the peak current density to that of large area devices to be about $2.5 \mu\text{m}^2$, similar to the conventional cross-wire devices.

Single photon counting experiments were carried out at 4.5 K in a cryogenic counting system.¹³ An attenuated 685

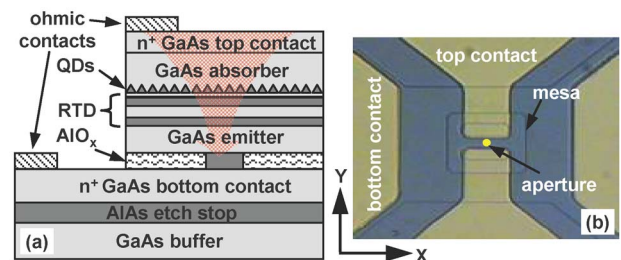


FIG. 1. (Color online) (a) Schematic diagram of the GaAs/AlAs QDRTD with oxide aperture. (b) Optical microscopy image of a device. The aperture is marked as a yellow (online) circle.

^{a)}Present address: Nokia Research Center, Cambridge, UK.

^{b)}Electronic mail: beka@fotonik.dtu.dk.

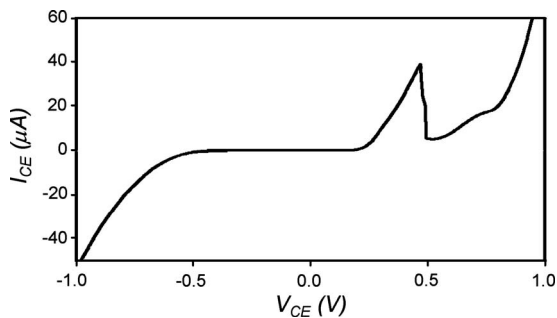


FIG. 2. Current-voltage characteristic of the device. Positive bias corresponds to the oxide aperture in the emitter of the device.

nm pulsed laser driven at 250 kHz was used as photon source. The following two 420 ns time windows were used for counting: one synchronized with the laser pulse and the other delayed by 2.0 μ s. The synchronized window counts both the photon-induced pulses and dark pulses while the delayed window counts only the dark pulses. Typical counting results as a function of discriminator level are shown in Fig. 3(a) for a photon flux of 0.32 photons/pulse. Despite the high dark count level in this device,¹⁴ there is a clear signal of photon-induced counts. The photon-induced count rate measured at a discriminator level of 18 mV varies linearly with photon flux up to the flux of 8 photons/pulse, as shown in Fig. 3(b). The operation of the detector in the single photon detection regime was confirmed by the slope of 0.98 of the linear fit (red line) to the data. The single photon detection efficiency from the fit is determined to be $2.1\% \pm 0.1\%$; at the same level as our previous cross-wire devices, which had, however, a 300 nm thick GaAs absorber.¹⁴ For the 100 nm absorber layer, we expect absorption efficiency of around 15%, yielding 14% internal quantum efficiency of our device.

In order to evaluate the effective absorption area of the device we measured position dependence of photon detection efficiency. Figure 4 shows the counting rate (in the time window synchronized with laser) at discriminator levels of 30 and 50 mV as a function of X axis scan [defined in Fig. 1(b)]. The origin of the plot corresponds to the center of the aperture, where the highest photon counting rate is recorded. The Gaussian detection peak at 30 mV has a width of about 1.87 μ m, and is superimposed on the constant background of the dark counts. The scan along Y axis gives similar results yielding the active photon collection area of 2.75 μ m². A scan at 50 mV is somehow different. The constant level of dark counts is lower and the Gaussian curve is narrower,

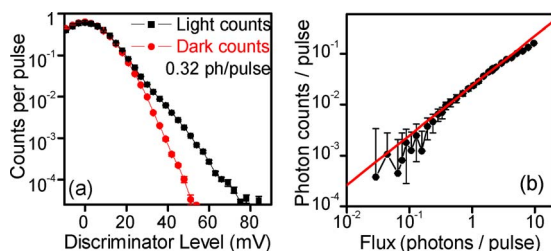


FIG. 3. (Color online) (a) Total (photon and dark counts) and dark count rates as a function of discriminator level under 685 nm illuminations at 0.32 photons/pulse. (b) Photon-induced counts as a function of laser pulse filling factor at a discriminator level of 18 mV (filled squares). The straight line is a linear fit of the data points.

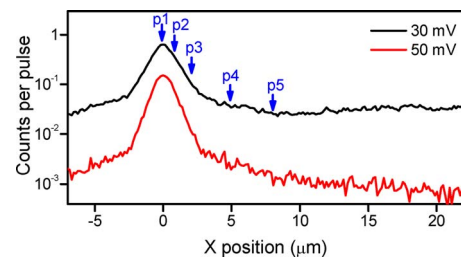


FIG. 4. (Color online) Counting rate as a function of X axial positions for discriminator levels of 30 and 50 mV. μ -PL spectra were taken at positions of p1–p5.

which is consistent with detector working in the two-photon detection regime. Additional slowly varying signal extending to 8 μ m can be seen on the background of the highly reduced dark counts. It suggests that a very small fraction of the photoholes generated in this region is focused toward the aperture.

In order to obtain insight into photohole paths in the absorber layer, which determines the optically active area of the detector, microphotoluminescence (μ -PL) from the InAs layer at positions p1–p5 (marked in Fig. 4) were recorded. The results are shown in Fig. 5. Figure 5(a) shows the bias dependence of μ -PL at p1 while Fig. 5(b) shows spectra at p1–p5 under 0.95 V bias. The bias marked in the figure is the total voltage applied in series with 10 k Ω resistor.¹³ In Fig. 5(a) at low biases, the PL signal is dominated by the emission from the wetting layer (peak at 855 nm) while at high biases discrete emission lines from individual QDs (extending to 940 nm) are strongest. The quenching of the luminescence at shorter wavelengths (e.g., wetting layer) as the bias increases is caused by fast carrier escape at higher electric field.

In Fig. 5(b), as the spot is moved away from the aperture, the wetting layer PL intensity becomes more pronounced. This change is equivalent to the trend with decreasing bias in Fig. 5(a). The PL spectrum at p5 with a strong wetting layer signal is similar to emission at 0.35 V at p1. This means that the potential at the collector side of the RTD is not sharply changing at the edge of the aperture so even outside the aperture (e.g., position p5) there is attractive potential for the photoholes. However, the capture of photoholes in the InAs layer is not detected electrically due to negligible tunneling current flowing in this area. This can be improved in future by redesigning the emitter of the device by bringing the oxide aperture closer to the RTD structure.

In conclusion, a single photon detector with an oxide aperture based QDRTD on GaAs substrate has been realized.

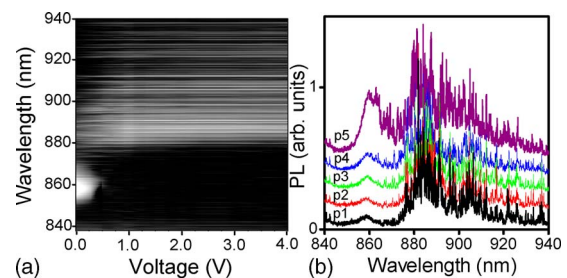


FIG. 5. (Color online) (a) Bias dependent μ -PL of position p1. White corresponds to high luminescence intensity, black to low. (b) μ -PL traces of positions p1–p5 under 0.95 V bias.

The device shows good electric characteristics and a single photon detection efficiency of $2.1\% \pm 0.1\%$ at 4.5 K at 685 nm wavelength. The light absorption area is similar to aperture size due to too small focusing electric field outside the aperture. Although further optimization of device geometry is needed to change the electric field distribution in the collector, this method of fabrication is easier, has higher yield, and results in more robust devices, compared with cross-wire device processing.

The authors would like to thank Dr. Daniel Granados at Toshiba Research Europe, Ltd., for help on μ -PL measurements. The authors would like to thank financial support from the Integrated Project SECOQC of the IST Priority (Sixth Framework) of the European Union.

¹N. Gisin, G. Ribordy, W. Tittel, and H. Zbinden, *Rev. Mod. Phys.* **74**, 145 (2002).

²C. Gobby, Z. L. Yuan, and A. J. Shields, *Appl. Phys. Lett.* **84**, 3762 (2004).

³J. Kim, S. Takeuchi, Y. Yamamoto, and H. H. Hogue, *Appl. Phys. Lett.* **74**, 902 (1999).

⁴G. N. Gol'tsman, O. Okunev, G. Chulkova, A. Lipatov, A. Semenov, K.

Smirnov, B. Voronov, A. Dzardanov, C. Williams, and R. Sobolewski, *Appl. Phys. Lett.* **79**, 705 (2001).

⁵S. Komiyama, O. Astafiev, V. Antonov, T. Kutsuwa, and H. Hirai, *Nature (London)* **403**, 405 (2000).

⁶A. J. Shields, M. P. O'Sullivan, I. Farrer, D. A. Ritchie, R. A. Hogg, M. L. Leadbeater, C. E. Norman, and M. Pepper, *Appl. Phys. Lett.* **76**, 3673 (2000).

⁷E. J. Gansen, M. A. Rowe, M. B. Greene, D. Rosenberg, T. E. Harvey, M. Y. Su, R. H. Hadfield, S. W. Nam, and R. P. Mirin, *Nat. Photonics* **1**, 585 (2007).

⁸J. C. Blakesley, P. See, A. J. Shields, B. E. Kardynal, P. Atkinson, I. Farrer, and D. A. Ritchie, *Phys. Rev. Lett.* **94**, 067401 (2005).

⁹H. W. Li, B. E. Kardynal, P. See, A. J. Shields, P. Simmonds, H. E. Beere, and D. A. Ritchie, *Appl. Phys. Lett.* **91**, 073516 (2007).

¹⁰A. J. Shields, M. P. O'Sullivan, I. Farrer, D. A. Ritchie, M. L. Leadbeater, N. K. Patel, R. A. Hogg, N. J. Curson, and M. Pepper, *Jpn. J. Appl. Phys., Part 1* **40**, 2058 (2001).

¹¹W. Wang, Y. Hou, D. Xiong, N. Li, W. Lu, W. Wang, H. Chen, J. Zhou, E. Wu, and H. Zeng, *Appl. Phys. Lett.* **92**, 023508 (2008).

¹²D. J. P. Ellis, A. J. Bennett, A. J. Shields, P. Atkinson, and D. A. Ritchie, *Appl. Phys. Lett.* **88**, 133509 (2006).

¹³B. E. Kardynal, A. J. Shields, N. S. Beattie, I. Farrer, K. Cooper, and D. A. Ritchie, *Appl. Phys. Lett.* **84**, 419 (2004).

¹⁴S. S. Hees, B. E. Kardynal, P. See, A. J. Shields, I. Farrer, and D. A. Ritchie, *Appl. Phys. Lett.* **89**, 153510 (2006).